Analyst

RSC Publishing

PAPER

View Article Online
View Journal | View Issue

Cite this: *Analyst*, 2013, **138**, 2483

A non enzymatic glucose biosensor based on an ultrasensitive calix[4]arene functionalized boronic acid gold nanoprobe for sensing in human blood serum†

Alok Pandya, Pinkesh G. Sutariya and Shobhana K. Menon*

We developed a new, advanced, simple and non enzymatic approach for the colorimetric detection of glucose based on calix[4]arene/phenyl boronic acid (CX-PBA)functionalized gold nanoparticles (AuNPs). This molecular receptor proficiently and selectively recognizes glucose due to its ability to reversibly bind diol-containing compounds. The assembly was characterized by transmission electron micrograph (TEM), dynamic light scattering (DLS), UV-Vis, FT-IR, ESI-MS and ^{1}H NMR spectrometry, which demonstrates the binding affinity for glucose *via* a boronic acid–diol interaction. The linear range for glucose was found to be 5–100 nM with phosphate buffer pH 10, with a lower detection limit of 4.3 nM. Interference by other saccharides was negligible. The biosensor has been successfully applied to estimate the glucose in human blood serum samples and the results compared well to an automatic analyzer. With the advantages of high sensitivity, selectivity and low sample volume, this method is potentially suitable for the on-site monitoring of glucose.

Received 11th December 2012
Accepted 16th February 2013

DOI: 10.1039/c3an36833e

www.rsc.org/analyst

1 Introduction

Sugars are essential biological molecules and consequently there is a high demand for blood glucose monitoring. Significant effort has been made in producing reliable glucose sensors for *in vitro* or *in vivo* applications,[1–7] as glucose can also plays elemental roles in controlling an individual's birth, differentiation and immunity.[7b] Diabetes is a widespread ailment that occurs due to large deviation of insulin in the body. More than 220 million of the world's population were affected by diabetes in the year 2011. Diabetes can damage the heart, nerves, eyes, kidneys and blood vessels.[8] Glucose in the blood is commonly used as the marker in clinical diagnosis, which is important to evaluate the health condition. So it is needed to develop a high selective and sensitive method for monitoring the D-glucose level in diagnostics. Traditional methods have been reported with enzyme based sensors or electrochemical methods for D-glucose monitoring.[9] Various techniques such as spectrophotometric,[10] electrochemical,[11–13] chemiluminescence,[14] fluorescence[15,16] and oxygen (O_2) sensor methods[17,18] have been reported. Most of these methods are based on the immobilization of the enzyme glucose oxidase (GOx) on a solid substrate which relies heavily on the properties of the supporting materials. They should provide a good environment for enzyme immobilization and should be able to maintain their biological activity. Gold nanoparticles (AuNPs) colorimetric biosensors have attracted particular interest in diagnostics and environmental monitoring. The functional mechanism for such biosensors derives from the aggregating behaviour of AuNPs.[19–22] In recent years, determination of D-glucose with nanoparticles has attracted great interest because of their special optical properties.[23,24] However, most of these methods involving nanoparticles are based on enzymes. Enzymes can be easily denatured by environmental changes or digested by proteases.[25]

In contrast, chemical sensors based on boronic acid have attracted much attention because of their greater stability and are widely used in the synthesis of sensors for carbohydrates and other diol containing compounds.[26–29] Such applications rely on the known thermodynamic and kinetic properties of boronic acid to form a tight complex with a diol moiety and are also studied in terms of the magnitude of the binding constants with various sugars and factors that affect binding. Phenyl boronic acids form stable cyclic esters with diol moieties of sugars in aqueous solution, which exhibit excellent selectivity due to two boronic acids possessing the proper spatial positioning and can selectively form a 2 : 1 complex with D-glucose.[30,31] As we know, supramolecular organizations, such as calix[4]arene, are ideal frameworks for molecular recognition because of their conformational and structural flexibility and their ability to be modified at both the upper

Department of Chemistry, School of Sciences, Gujarat University, Ahmedabad, Gujarat-380009, India. E-mail: shobhanamenon07@gmail.com; Fax: +91 79 26308545; Tel: +91 79 26302286

† Electronic supplementary information (ESI) available: The synthetic procedure associated with this article can be found in the ESI. See DOI: 10.1039/c3an36833e

and lower rims. So, the modified calix[4]arene at the lower rim can show some specific and excellent properties when they are appropriately functionalized. As mentioned above, here we have been investigating the calixarene/phenyl boronic acid complex because calix[4]arene can accommodate the phenyl boronic acid probe and they catch D-glucose with high selectivity. Recently, we reported potassium ion recognition by benzo-15-crown-5 Au nanoparticles,[32] selective amino acid recognition of lysine, arginine and histidine by functionalized calix[4]arene thiol AuNPs,[33] the rapid colorimetric detection of sulfide using calix[4]arene modified gold nanoparticles[34] and a novel nanoaggregation detection technique of TNT using selective and ultrasensitive nanocurcumin.[35] The sensitivity and selectivity of these sensors prompted us to design and develop a D-glucose biosensor.

In this paper, we designed a new promising approach using AuNPs based on a colorimetric sensing system (ANCSS) which forms calix[4]arene boronic acid functionalized gold nanoprobe complexes (CX-BA–AuNPs) for the detection of D-glucose (Glu) in water. In this work, a closed chamber of a microwave system with precise temperature control function was employed to synthesize the gold nanoparticles. In the microwave assisted method, the nanomaterial can be selectively heated preferentially in comparison to the solvent and ligand.[36] This sensor is based on *p*-suphonato-25,28 diethoxy [4-sulfanyl methyl] phenyl boronic acid calix[4]arene (pSC$_4$BA) and gold nanoparticles (Scheme 1). The AuNPs[34] and *p-tert*-butylcalix[4]arene were synthesized by microwave assisted method.

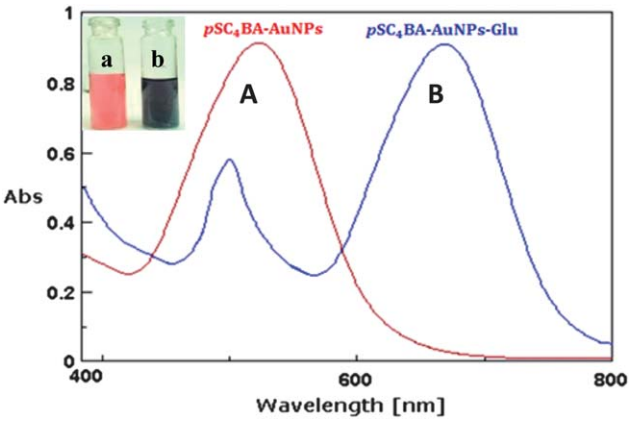

Fig. 1 UV-Vis spectra and photo images of (A) pSC$_4$BA–AuNPs without D-glucose (B) pSC$_4$BA–AuNPs with 25 nM D-glucose concentration (pSC$_4$BA–AuNPs–Glu).

2 Materials and methods

All chemicals used were of the highest purity available. All solutions were prepared with deionized water. HAuCl$_4$, glucose, fructose, sucrose, lactose, mannose, vitamin C and citric acid were purchased from Aldrich. Silica gel (Merck, 0.040–0.063 mm) was used for the column chromatography. Working standard solutions were prepared daily in deionised water. To study the effect of pH, 0.025 M potassium dihydrogen orthophosphate (KH_2PO_4) buffer solution was added into 0.2% orthophosphoric acid to get a pH from 3.5 to 6.5 and to make basic

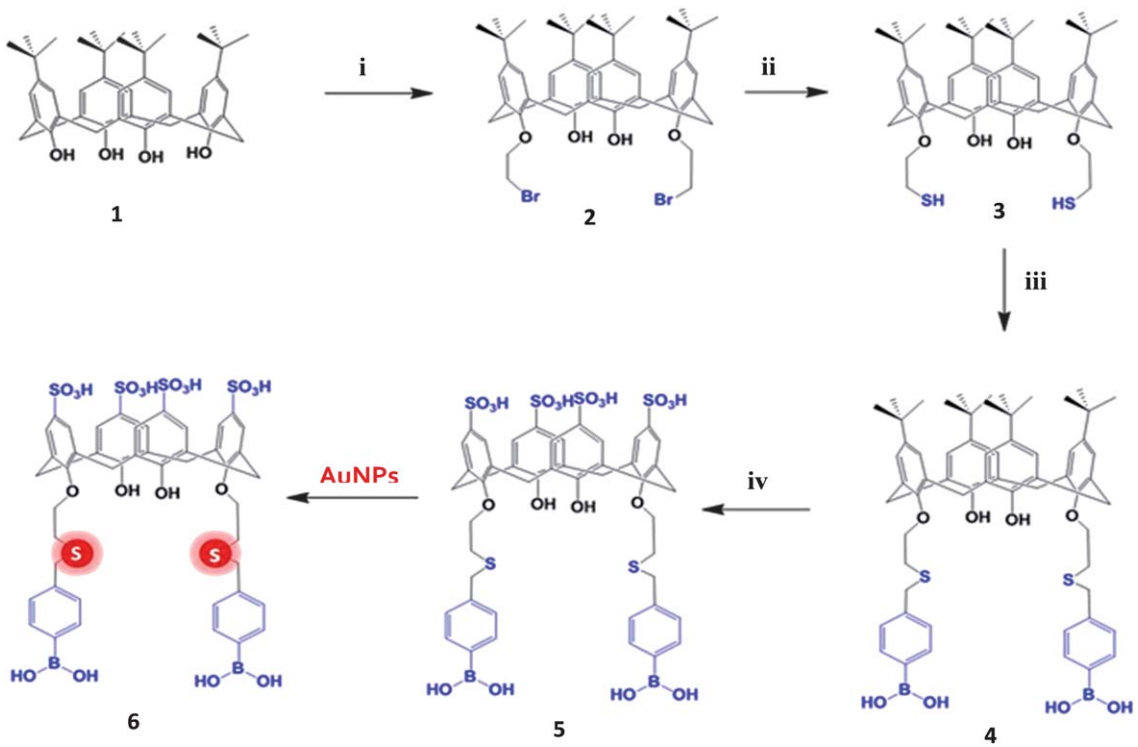

Scheme 1 Synthesis of pSC$_4$BA–AuNPs ligand. *Reagents and conditions*: (i) dibromoethane, K_2CO_3, reflux, 18 h, (ii) thiourea, NaOH, 48 h, (iii) 4-bromomethyl phenyl boronic acid, K_2CO_3, reflux, 18 h, (iv) con. H_2SO_4, 50 °C.

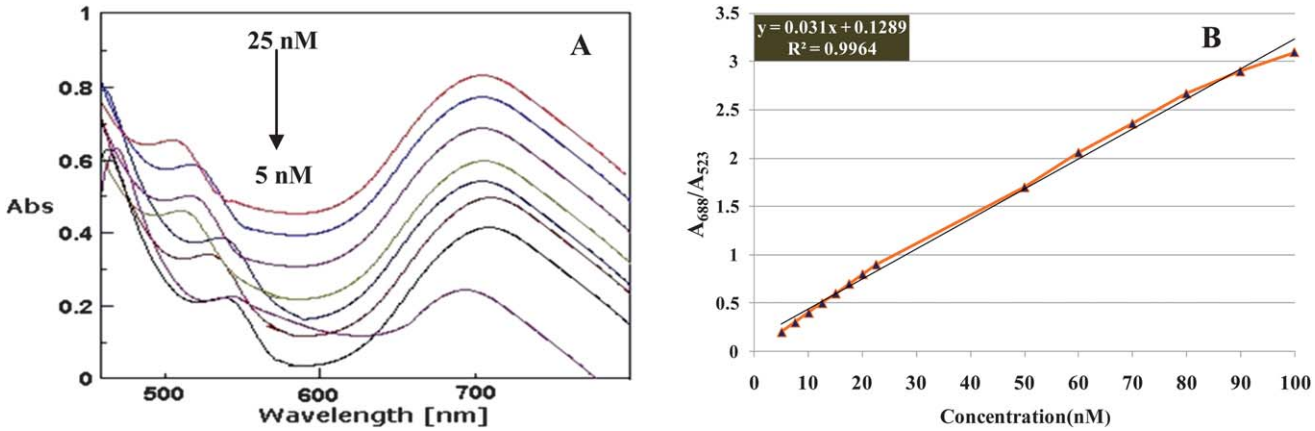

Fig. 2 (A) UV-Visible spectra obtained from solutions of 0.21 mM gold responding to various concentrations of D-glucose. The curves from bottom to top show gradually increasing concentrations of sulfide ion: (a) 5 nM (b) 7 nM (c) 10 nM (d) 12 nM (e) 15 nM (f) 17 nM (g) 20 nM (h) 25 nM. (B) Linear correlation between the absorbance and D-glucose pH 10.0 adjusted by Na_2C0_3–H_3PO_4, buffer, 25 °C.

pH, 0.025 M potassium dihydrogen orthophosphate (KH_2PO_4) buffer solution was added into 0.2% Na_2CO_3 to maintain the pH (8–12). UV-Vis absorption spectra were acquired on a Jasco V-570 UV-Vis spectrometer. IR spectra were measured with a Bruker Tensor 27 FT-IR spectrometer. Transmission electron micrographs (TEM) were recorded by JEOL, JEM-2100 (200 kV). ^{1}H NMR was carried out in $CDCl_3$ (TMS for internal standard) on a Bruker, Avance II (500 MHz). Dynamic light scattering (DLS) measurements were performed using a Nanotrac instrument. The pH measurements were made by using model EQ-664 (Equiptronics).

2.1 Glucose sensing using *p*SC_4BA functionalized gold nanoparticles

The stock solution of glucose (0.01 M) was prepared by dissolving glucose (1.80 g) in deionized water and was diluted to 5 nM, 10 nM, 50 nM, 100 nM, 1 μM and 0.1 mM and was detected by a 0.21 mM solution of *p*SC_4BA–AuNPs. To detect glucose, 1 mL of 0.1 mM glucose was added into 4 mL of 0.21 mM *p*SC_4BA–AuNPs with 2 mL of phosphate buffer (pH 10) and marked up to 10 mL. The shift in the surface plasmon resonance (SPR) absorption maxima of the *p*SC_4BA–AuNPs on adding predetermined quantities of glucose standard was recorded using a UV-Visible absorption spectrophotometer and a calibration curve was plotted with the wavelength against the optical density. The human blood samples were collected from a local hospital. The corresponding shift in the absorption maxima was used to calculate the amount of glucose present.

3 Results and discussion

3.1 Glucose recognization studies

3.1.1 UV-Visible spectrophotometry. The surface plasmon resonance makes the absorption cross-section of the nanoparticles several orders of magnitude stronger than the most strongly absorbing molecules and the light scattering cross-section several orders of magnitude stronger than the organic dyes with a high extinction coefficient. Thus, most of the applications of the AuNPs as sensors are based on detecting the shift in surface plasmon peak, either due to a change in the local dielectric constant of the nanoparticles by adsorbed biomolecules, or due to analyte induced aggregation of the nanoparticles. Both of these effects rely on the selectivity provided by the functionalized capping agents. We investigated spectrophotometrically the UV-Vis spectrum of the calix capped AuNPs solution, which shows an absorption maximum at 523 nm. After several months of storage, the calixarene capped AuNPs surface plasmon band wavelengths remained the same, which indicates that microwave synthesized nanoparticles are

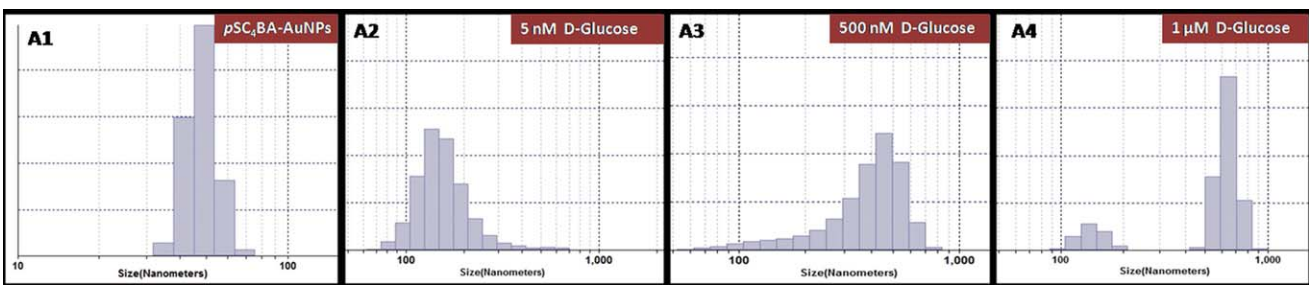

Fig. 3 Size distribution of *p*SC_4BA conjugated AuNPs measured by DLS. (A1) In the absence of glucose (*p*SC_4BA–AuNPs) (A2) in the presence of 5 nM D-glucose (A3) 500 nM D-glucose and (A4) 1 μM D-glucose.

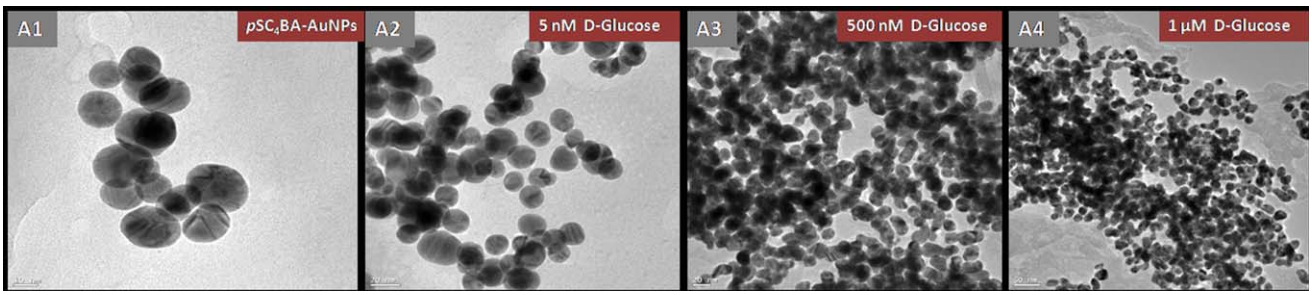

Fig. 4 TEM images showing how pSC_4BA–AuNPs aggregate sizes vary in response to the addition of different concentrations of D-glucose (A1) in the absence of glucose (pSC_4BA–AuNPs) (A2) in the presence of 5 nM D-glucose (A3) 500 nM D-glucose and (A4) 1 μM D-glucose.

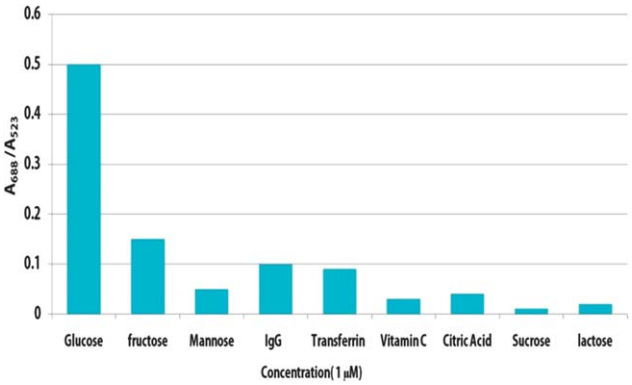

Fig. 5 The relative absorbance change of pSC_4BA–AuNPs at 523 nm in the presence of 1 μM D-glucose over other saccharides.

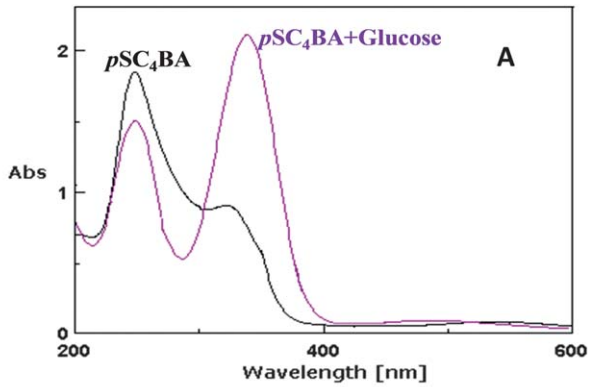

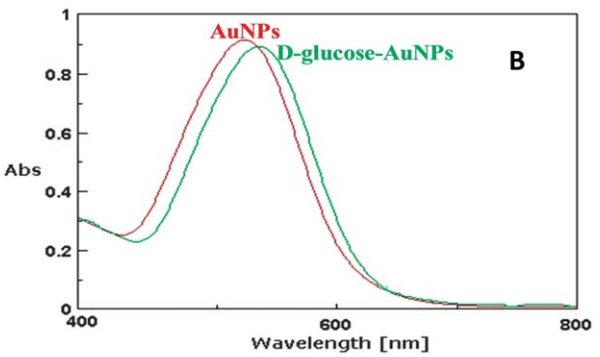

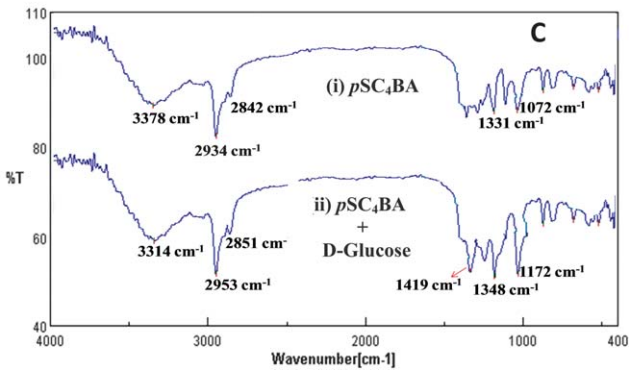

Fig. 6 (A) UV-Vis spectra as a function of the interaction of pSC_4BA with D-glucose concentration and (B) UV-Vis spectra of the interaction of AuNPs with D-glucose (C) FT-IR spectra as a function of the interaction of pSC_4BA with D-glucose concentration, pH 10.0 adjusted by buffer Na_2CO_3–H_3PO_4, *T*-2 min, 25 °C.

stable. The calix capped AuNPs are miscible with water and the solution without D-glucose is a wine red colour. Fig. 1 shows the surface plasma resonance and photo images of AuNPs without (a) and with (b) D-glucose. In the absence of D-glucose, the AuNPs were wine red and displayed an intense surface plasma band at about 523 nm. While in the presence of 25 nM D-glucose, the absorbance of AuNPs at 523 nm decreased and a new peak appeared at about 688 nm and the color of AuNPs changed from wine red (a) to blue (b), indicating the state of AuNPs changed from mono-dispersed to aggregated (Fig. 1B).

3.1.2 Sensitive colorimetric detection of D-glucose. To examine this simple assay for the direct colorimetric determination of D-glucose, UV-Visible spectra were recorded in the absence and presence of different concentrations of D-glucose. As we know, the color of 0.21 mM pSC_4BA–AuNPs was wine red and displayed a characteristic absorption band at 523 nm (Fig. 1A). However, a color change to blue took place due to aggregation and a significant change in the spectral profile was noticed upon the gradual addition of different concentrations of D-glucose from 25 nM to 5 nM with 0.21 mM pSC_4BA–AuNPs. These changes were as follows: (a) a gradual decrease in the surface plasmon resonance at about 523 nm (b) appearance of a new band at about 688 nm (c) a slight red shift and gradual increase in the surface plasmon resonance at about 688 nm (Fig. 1B) and which were ascribed to the aggregation of AuNPs and exhibit selective binding with D-glucose *via* interaction of

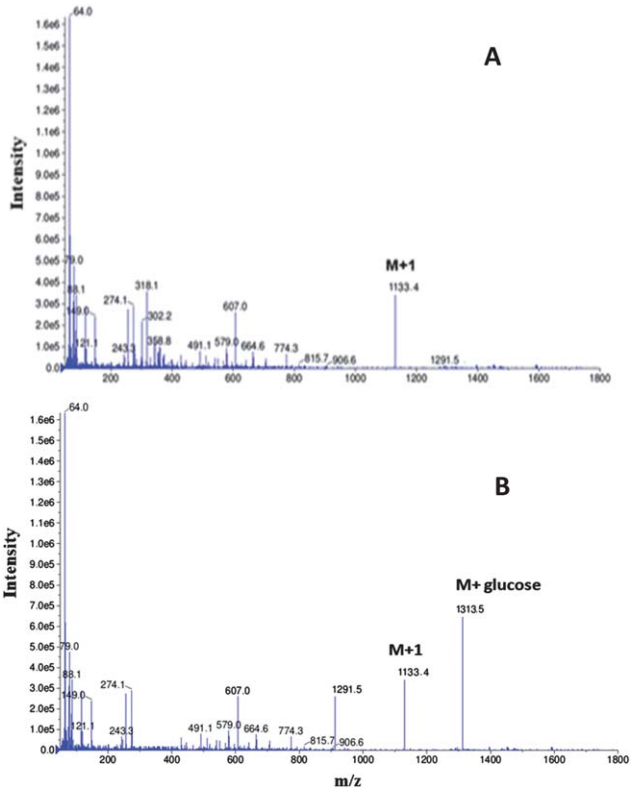

Fig. 7 ESI-MS spectra of the mixtures of (A) pSC$_4$BA–AuNPs (B) pSC$_4$BA–AuNPs–Glu.

the boronic acid–diol with glucose (pSC$_4$BA–AuNPs–Glu). Prominently, it was found that even the addition of a low concentration of D-glucose could lead to an obvious color change which could be distinguished with the naked eye. The absorption ratio A_{688}/A_{523} was used to quantify the concentration of D-glucose. It is concluded that the change in solution color and degree of red shift are associated with the increase in the size of aggregated nanoparticles (Fig. 2A). It is directly noticeable that there is significant change in absorbance intensity at 523 nm upon increasing concentration of the D-glucose. However after 4 days color intensity decreases very slowly due to sedimentation. The linear range for D-glucose, using 0.21 mM pSC$_4$BA–AuNPs was found to be 5–100 nM (R^2 = 0.996) (Fig. 2B). The lower detection limit was found to be 4.3 nM, which is a higher sensitivity than previously reported methods.[11–13,23–25]

3.1.3 The effect of the reaction time. As shown in Fig. S1 (see ESI†) the absorption ratio (A_{688}/A_{523}) remained unchanged after 4 min, indicating the interaction was almost completed under this condition. Therefore, all the absorption measurements were performed in 2 min.

3.2 Dynamic light scattering measurements

To evaluate the aggregation of pSC$_4$BA–AuNPs–Glu, we have employed pSC$_4$BA attached AuNPs based DLS analysis. The dynamic light scattering (DLS) technique illustrates that before surface modification, the AuNPs had an average diameter of ~38 nm, which maintained their size and stability. After ligand exchange, the pSC$_4$BA coating on AuNPs increased the average hydrodynamic diameter to ~45 nm (Fig. 3A1) which is close to the average hydrodynamic diameter of AuNPs. In contrast, upon addition of different D-glucose concentrations (5 nM, 500 nM, 1 μM), pSC$_4$BA–AuNPs agglomerated and the size increased to (~126 nm, ~460 nm, ~854 nm) respectively (Fig. 3A2–A4). Thus, a pSC$_4$BA conjugated AuNPs based DLS assay should be able to show a response at a lower concentration of glucose with only smaller aggregates formed, and at higher concentrations of glucose shows bigger aggregates might be due to dimer formation between D-glucose and boronic acid.

3.3 TEM analysis

To appraise the aggregation of pSC$_4$BA–AuNPs–Glu further we have studied the pSC$_4$BA attached AuNPs based TEM measurements. The TEM micrograph for the typical sample of pSC$_4$BA–AuNP shows the complexes were completely discrete with a mean diameter of ~45 nm (Fig. 4A1), but after addition of different concentrations (5 nM, 500 nM, 1 μM) of D-glucose into pSC$_4$BA–AuNPs, the TEM measurements indicate aggregate formation of the pSC$_4$BA–AuNPs due to boronic acids forming complexes with the D-glucose (Fig. 4A2–A4).

3.4 Selectivity of the assay

The selectivity of the assay was evaluated with other analytes such as fructose, sucrose, lactose, mannose, vitamin C, citric acid and glycoproteins, such as IgG and transferrin, at a concentration of 1 μM for the determination of 1 μM glucose in the presence of 0.21 mM pSC$_4$BA–AuNPs. The experimental results are shown in Fig. 5, it is clear that only D-glucose showed a higher absorption ratio (A_{688}/A_{523}), confirming the excellent selectivity of the proposed assay to D-glucose. Glycoproteins can interfere due to their binding ability with boronic acids, but this can be avoided by finely tuning the pH range to 8–10.[37] For a given diboronic acid containing scaffold, the spacing between the boronic acids could be attuned through synthetic modifications in order to build a glucose-specific binding pocket compared to other significant monosaccharides, such as fructose.[38,39]

3.5 Effect of pH

We also examined the stability of the pSC$_4$BA–AuNPs assembly at different pH conditions (Table S1, see ESI†). It was perceived that pSC$_4$BA–AuNPs exhibited stability in slightly acidic solution (pH 2 to pH 7) and remained more stable in the range of pH of 7 to 10 for weeks to months, with no sign of further aggregation. Furthermore, the pSC$_4$BA–AuNPs assembly displays a high stability at room temperature with no sign of aggregation.

3.6 D-Glucose binding mechanism

In studying the phenyl boronic acid based glucose binding processes, it is important to have a general understanding of the structural properties of boronic acid and the steps involved in boronic acid binding to a diol. It is well known that boronic

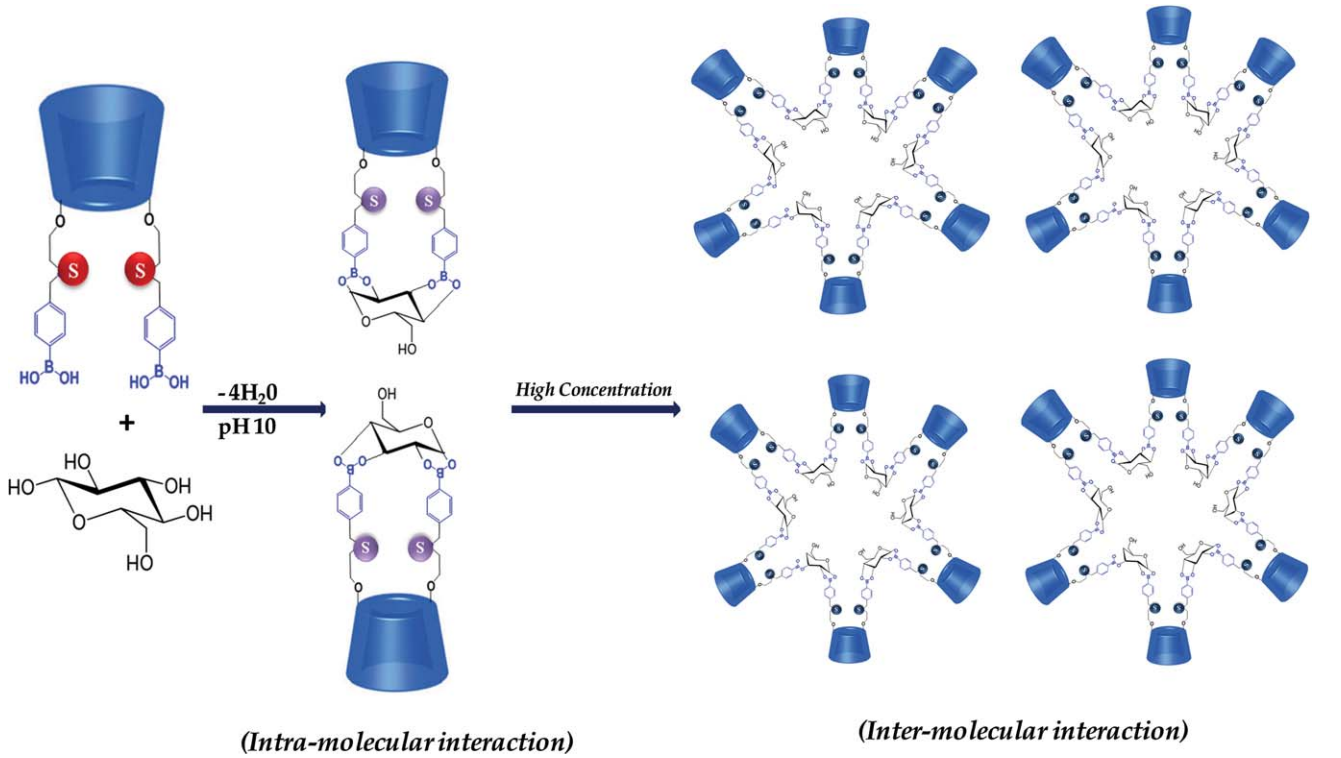

Fig. 8 Schematic of the glucose sensing with pSC$_4$BA modified AuNPs *via* nanoaggregation due to specific intramolecular or intermolecular interaction between pSC$_4$BA–AuNPs and glucose.

acids are weak Lewis acids due to the open shell on the boron atom and the reaction with a protic solvent molecule, such as water to yield the tetrahedral boronate while releasing a proton, which is also responsible for the ability of boronic acid to bind reversibly with diols,[40] other acids[41,42] and Lewis bases.[43] Thus, when we investigated spectrophotometrically, experimental observation indicated that the bathochromic shift is observed during the interaction of the pSC$_4$BA–AuNPs with D-glucose, which is due to existence of the boronic acid–diol binding complex.

In order to confirm a boronic acid–diol binding process during glucose complexion with pSC$_4$BA, the UV-Visible experiments were performed with uninteracted 0.2 mM pSC$_4$BA **5** and the absorption maximum was observed at 259 nm. But interestingly, after interaction of D-glucose with 0.2 mM pSC$_4$BA the absorption maximum shifted to 265 nm and 341 nm (Fig. 6A). These observations suggested that the appearance of the new sharp absorption peak maximum is due to the rapid formation of the boronic acid–diol complex. The simple *p-tert*-butyl dibromoethoxy calix[4]arene, *p-tert*-butyl dithioethoxycalix[4] arene do not show any change in absorption maximum. Furthermore, we also evaluated the interaction of AuNPs with D-glucose ions by UV-Vis spectroscopy which shows a decrease in the absorbance and broadening with a small shift in the absorption maximum owing to strong chemisorptions (Fig. 6B).

The binding mechanism of glucose with pSC$_4$BA–AuNPs was further evidenced by FT-IR spectroscopy. Fig. 6C shows the FTIR spectra in the region of 4000 to 400 cm^{-1} for both species. The most notable modes from glucose are the C–O stretching band centered at 1072 cm^{-1} with several modes with a C–O stretching component in the 850–1180 cm^{-1} region, C–C stretching at 1331 cm^{-1} and the O–H stretching mode centered at 3378 cm^{-1} (Fig. 6C(i)). Then the spectra of glucose bound to pSC$_4$BA–AuNPs shows a shift in the O–H stretching mode from 3378

Table 1 Determination and recovery of glucose in blood serum samples using the pSC$_4$BA–AuNPs glucose biosensor

Blood serum sample	Concentration of glucose (mmol L^{-1})[a]	Concentration of glucose (mmol L^{-1})[b]	RSD[c] (%)	Glucose added (mmol L^{-1})	Glucose found (mmol L^{-1})	Recovery (%)	RSD[c] (%)
1	3.1	2.9	0.75	5.0	8.0	99.5	0.95
2	3.4	2.1	1.43	5.0	7.9	96.7	1.31
3	5.8	5.3	1.12	5.0	10.4	98.9	1.01
4	6.9	6.6	0.98	5.0	11.5	99.4	0.88

[a] Determined by local hospital. [b] Determined by the pSC$_4$BA–AuNPs glucose biosensor. [c] Three replicates were performed.

cm^{-1} of the pSC_4BA–AuNPs to 3314 cm^{-1} of the O–H stretching mode of glucose bound to pSC_4BA–AuNPs due to the O–H stretching mode of glucose coming closer due to aggregation. After binding of the glucose with pSC_4BA–AuNPs, the B–O stretching modes (1419 cm^{-1}, 1348 cm^{-1}), C–O stretching (1172 cm^{-1}) is observed (Fig. 6C(ii)). The B–O stretching modes are shifted with a different peak profile with glucose bound to pSC_4BA–AuNPs (phenyl boronate ester) compared to pSC_4BA–AuNPs without glucose bound (phenyl boronic acid). The C–O stretching mode of glucose is also evident in the glucose bound to pSC_4BA–AuNPs. These observations are solid evidence of the formation of a phenyl boronate ester with glucose (pSC_4BA–AuNPs–Glu). The acid/diol based complex formation between pSC_4BA–AuNPs and glucose was further confirmed by ESI-MS spectroscopy. Fig. 7 shows the ESI-MS spectra of the mixtures of pSC_4BA–AuNPs and glucose with pSC_4BA–AuNPs in aqueous solution. The spectra of pSC_4BA–AuNPs shows a peak at m/z = 1133.4 (Fig. 7A).

When the glucose was mixed with pSC_4BA–AuNPs in aqueous solution, a pSC_4BA–AuNPs–Glu peak at m/z = 1313.5 was clearly detected (Fig. 7B), which undoubtedly suggests the formation of boronic acid–diol complexation through covalent bonding.

To monitor the effect of the pH of the medium, the adsorption measurements were carried out at pH values 3, 7 and 10 respectively. Many scientists have made efforts to reduce the pH of boronic acids or boronic acids-functionalized materials for binding with sugars or glycoproteins.[44–50] In our present method, we also evaluated the pSC_4BA–AuNPs assembly in the pH range of 7.5–10 (Fig. S2, see ESI†). At pH 3 to 6 the absorption maximum value was observed at 523 nm, unchanged from the control test results. At pH 7.5 to 10, the plasmon band shifted to 688 nm. The high complexation between boronic acid and the diol of glucose is dependent on pH, having a high intensity obtained at pH 7.5 to 10. As discussed earlier, boronic acid can exist in two states: neutral trigonal and tetrahedral anionic forms. Depending on the pK_a of the boronic acid and solution pH, the ratio of these two forms changes. Such a result robustly proves that D-glucose binds more tightly with phenyl boronic acids *via* intra-molecular or intermolecular interaction (Fig. 8).

3.7 Glucose analysis from human blood serum

To exemplify the feasibility of the pSC_4BA–AuNPs based glucose biosensor in practical analysis, it was employed to measure glucose in human blood serum. The concentration of glucose in human blood serum is from 3.9 to 6.1 mmol L^{-1} for most healthy subjects. Fresh human blood samples were collected in a local hospital and analyzed by both the spectrophotometric method and pSC_4BA–AuNPs based glucose biosensor. In our work, the blood serum samples were simply diluted at pH 10, the precipitation was filtered and used for detection. The absorbed glucose component was diluted up to 10 100 fold and analyzed by the present method and the results are shown in Table 1 with a quantitative recovery up to 99.5%. The analysis and recovery test results of the calix capped gold nanoparticles demonstrate that the glucose biosensor offers an excellent, accurate, fast and precise method for the determination of glucose in human blood serum.

4 Conclusion

In this work, we proposed a novel approach for a stable and highly sensitive glucose biosensor which has been successfully made-up using pSC_4BA–AuNPs. The plasmon absorption peak was red-shifted proportionally for up to 5 nM glucose, and a good correlation was obtained between the wavelength shift and concentration pointing out the feasibility of the method for the quantitative measurement of glucose with a lower detection limit of 4.3 nM. It is easy to operate and, most importantly, it exhibits a fast response time (<60 s) to glucose and has a long shelf-life (>5 weeks). The developed pSC_4BA–AuNPs based glucose biosensor has been proven to be a simple, reliable and accurate tool for the determination of glucose in human blood serum. Further, we extend this work to make a strip for the detection of glucose which is still ongoing.

Acknowledgements

Financial assistance from UGC, New Delhi is gratefully acknowledged.

References

1 B. Rabinovitch, W. F. March and R. L. Adams, *Diabetes Care*, 1982, **5**, 254–258.
2 I. J. Hatoum, F. B. Hu, J. J. Nelson and E. B. Rimm, *Diabetes*, 2010, **59**, 1239–1243.
3 A. N. Kollias and M. U. Ulbig, *Ärztt. Inter.*, 2010, **107**, 75–84.
4 A. H. Salanitro and C. L. Roumie, *Clinical Diabetes*, 2010, **28**, 107–114.
5 M. Free and H. Free, *Anal. Chem.*, 1984, **56**, 664A.
6 G. Reach and G. S. Wilson, *Anal. Chem.*, 1992, **64**, 381A.
7 (*a*) C. F. Brewer, M. C. Miceli and L. G. Baum, *Curr. Opin. Struct. Biol.*, 2002, **12**, 616–623; (*b*) S. Brodesser, P. Sawatzki and T. Kolter, *Eur. J. Org. Chem.*, 2003, 2021–2034.
8 World Health Organization, http://www.who.int/media-centre/factsheets/fs312/en/.2011.
9 L. Clark Jr and C. Lyons, *Ann. N. Y. Acad. Sci.*, 1962, **102**, 29–45.
10 A. X. Han, G. S. Wu, Q. Liang and F. S. Zhang, *Chin. J. Anal. Chem.*, 2003, **31**, 1417–1420.
11 T. Kong, Y. T. Chen, Y. P. Ye, K. Zhang, Z. X. Wang and X. P. Wang, *Sens. Actuators, B*, 2009, **138**, 344–350.
12 X. L. Luo, J. J. Xu, Y. Du and H. Y. Chen, *Anal. Biochem.*, 2004, **334**, 284–289.
13 R. B. Rakhi, K. Sethupathi and S. Ramaprabhu, *J. Phys. Chem. B*, 2009, **113**, 3190–3194.
14 X. Q. Liu, W. X. Niu, H. J. Li, S. Han, L. Z. Hu and G. B. Xu, *Electrochem. Commun.*, 2008, **10**, 1250–1253.
15 J. Galbán, Y. Andreu, M. J. Almenara, S. De Marcos and J. R. Castillo, *Talanta*, 2001, **54**, 847–854.
16 V. Sanz, J. Galban, S. De Marcos and J. R. Castillo, *Talanta*, 2003, **60**, 415–423.
17 B. L. Wu, G. M. Zhang, S. M. Shuang and M. M. F. Choi, *Talanta*, 2004, 546–553.
18 Y. Zhang, G. M. Wen, Y. H. Zhou, S. M. Shuang, C. Dong and M. M. F. Choi, *Biosens. Bioelectron.*, 2007, **22**, 1791–1797.

19 K. Aslan, J. R. Lakowicz and C. D. Geddes, *Anal. Biochem.*, 2004, **330**, 145–155.
20 H. Liu, D. Chen, L. Yang, X. Ren, F. Tang and J. Ren, *Nanotechnology*, 2010, **21**, 185504–185510.
21 S. Lee and V. H. Perez Luna, *Anal. Chem.*, 2005, **77**, 7204–7211.
22 F. W. Campbell and R. G. Compton, *Anal. Bioanal. Chem.*, 2009, **396**, 241–259.
23 S. Manju and K. Sreenivasan, *Talanta*, 2011, **85**, 2643–2649.
24 C. Radhakumary and K. Sreenivasan, *Anal. Chem.*, 2011, **83**, 2829–2833.
25 H. Wei and E. Wang, *Anal. Chem.*, 2008, **80**, 2250–2254.
26 S. J. Baker, T. Akama, Y. K. Zhang, V. Sauro, C. Pandit, R. Singh, M. Kully, J. Khan, J. J. Plattner, S. J. Benkovic, V. Lee and K. R. Maples, *Bioorg. Med. Chem. Lett.*, 2006, **16**, 5963.
27 S. J. Baker, Y. K. Zhang, T. Akama, A. Lau, H. Zhou, V. Hernandez, W. Mao, M. R. Alley, V. Sanders and J. J. Plattner, *J. Med. Chem.*, 2006, **49**, 4447.
28 H. S. Cao and M. D. J. Heagy, *J. Fluoresc.*, 2004, **14**, 569.
29 Y. Cheng, N. Ni, W. Yang and B. Wang, *Chem.–Eur. J.*, 2010, **16**, 13528.
30 S. Gamsey, A. Miller, M. M. Oimstead, C. M. Beavers, L. C. Hirayama, S. Pradhan, R. A. Wessling and B. Singaram, *J. Am. Chem. Soc.*, 2007, **129**, 1278–1286.
31 V. V. Karnati, X. Gao, S. Gao, W. Yang, W. Ni, S. Sankar and B. Wang, *Bioorg. Med. Chem. Lett.*, 2002, **12**, 3373–3377.
32 G. Patel, A. Kumar, U. Pal and S. Menon, *Chem. Commun.*, 2009, 1849–1851.
33 G. Patel and S. Menon, *Chem. Commun.*, 2009, 3563–3565.
34 A. Pandya, K. V. Joshi, N. R. Modi and S. K. Menon, *Sens. Actuators, B*, 2012, **168**, 54–61.
35 A. Pandya, H. Goswami, A. Lodha and S. K. Menon, *Analyst*, 2012, **137**, 1771–1774.
36 J. A. Gerbec, D. Magana, A. Washington and G. F. Strouse, *J. Am. Chem. Soc.*, 2005, **127**, 15791–15800.
37 J. Gross, J. H. Highberger and F. Schmitt, *Biochemistry*, 1955, **41**, 1.
38 N. Ni, S. Laughlin, Y. Wang, Y. Feng, Y. Zheng and B. Wang, *Bioorg. Med. Chem.*, 2012, **20**, 2957–2961.
39 G. Springsteen and B. Wang, *Tetrahedron*, 2002, **58**, 5291.
40 C. W. Gray Jr and T. A. J. Houston, *J. Org. Chem.*, 2002, **67**, 5426.
41 B. D. Smith, S. J. Gardiner, T. A. Munro, M. F. Paugam and J. A. J. Riggs, *J. Inclusion Phenom. Mol. Recognit. Chem.*, 1998, **32**, 121.
42 T. A. Houston, S. M. Levonis and M. J. Kiefel, *Aust. J. Chem.*, 2007, **60**, 811.
43 L. I. Bosch, T. M. Fyles and T. D. James, *Tetrahedron*, 2004, **60**, 11175.
44 G. Wulff, *Pure Appl. Chem.*, 1982, **11**(54), 2093–2102.
45 H. Y. Li, Y. Liu, J. Liu and Z. Liu, *Chem. Commun.*, 2011, **47**, 8169–8172.
46 M. Dowlut and D. G. Hall, *J. Am. Chem. Soc.*, 2006, **128**, 4226–4227.
47 L. B. Ren, Z. Liu, Y. C. Liu, P. Dou and H. Y. Chen, *Angew. Chem., Int. Ed.*, 2009, **48**, 6704–6707.
48 H. Y. Li, Y. Liu, J. Liu and Z. Liu, *Chem. Commun.*, 2012, **48**, 4115–4117.
49 Y. C. Liu, L. Ren and Z. Liu, *Chem. Commun.*, 2011, **47**, 5067–5069.
50 L. Liang and Z. Liu, *Chem. Commun.*, 2011, **47**, 2255–2257.

